Fifth International Penguin Conference
Ushuaia, Tierra del Fuego, Argentina

Automated Visual Recognition of Individual African Penguins

Tilo Burghardt,

Barry Thomas, Peter J Barham, Janko Ćalić

University of Bristol, Department of Computer Science,

MVB Woodland Road, Bristol BS8 1UB, United Kingdom,

September 2004

burghard@cs.bris.ac.uk

Abstract

African penguins *(Spheniscus demersus)* carry a pattern of black spots on their chests that does not change from season to season during their adult life. Further, as far as we can tell, no two penguins have exactly the same pattern. We have developed a real-time system that can confidently locate African penguins whose chests are visible within video sequences or still images. An extraction of the chest spot pattern allows the generation of a unique biometrical identifier for each penguin. Using these identifiers an authentication of filmed or photographed African penguins against a population database can be performed. This paper provides a detailed technical description of the developed system and outlines the scope and the conditions of application ∎
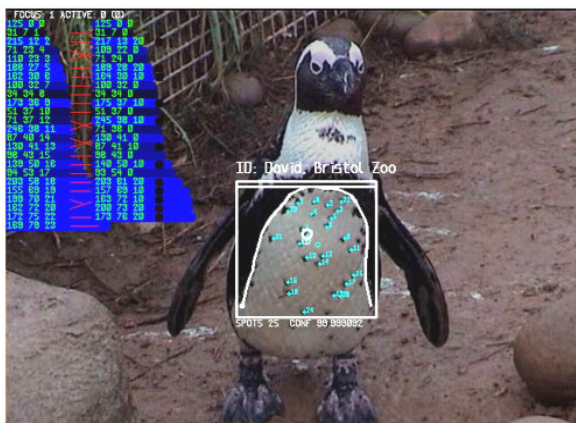
1. Introduction

At present when researchers want to identify individual penguins they use either flipper bands or in some cases transponders. In general, transponders are less useful as the bird carrying the device has to pass close enough to a reader before its presence can be noted. Transponders are invisible, being fitted internally. They do not provide immediate visual identification. For most practical purposes, a bird wearing a transponder still requires an identifying tag to indicate the transponder's presence – certainly something like a flipper band [15]. Flipper bands while much more visible are, possibly, harmful to the birds. The extent to which flipper bands impair penguins is still open to question, but it is widely believed there are at least some detrimental effects of wearing such bands.
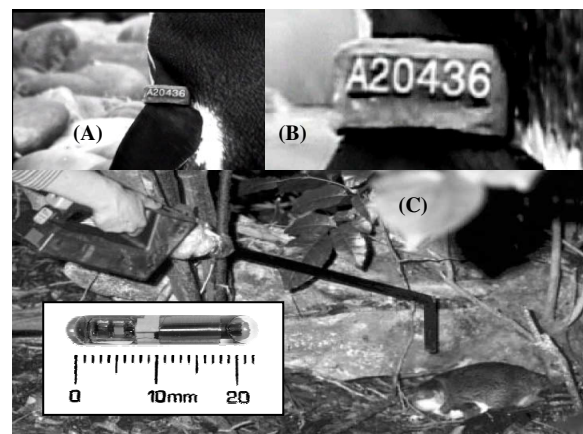

Figure 1. *Identification of an African Penguin by its Chest Pattern:* Screenshot of Software Prototype; African penguins carry a unique pattern of black spots on their chest. The detection of the chest location and the decomposition of the spot pattern allow checking a photographed individual (here penguin 'David' from Bristol Zoo) against a population database. (figure source [18], [19])

Figure 2. *The Classical Identification Methods for Penguins:* **(A)** African penguin with metal flipper band; **(B)** Close-up of a flipper band with registration number; **(C)** The TIRIS™ transponder, 23x4mm in size and 6g weight, can be used as implant to recognise penguins via short distance reading. The image shows transponder and reading procedure. (figure source [14], [18])

We have noted that all adult African penguins carry a pattern of black spots on their chests that do not change from season to season.

Further, as far as we can tell no two penguins have exactly the same pattern. Indeed many zoos use the unique spot pattern as a means of identifying the individuals in their collections.
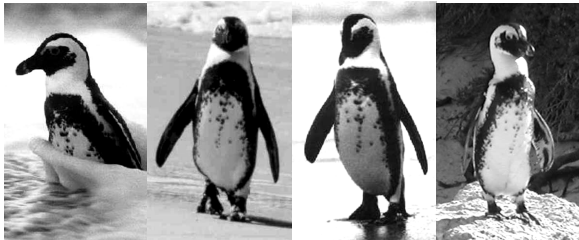

Figure 3. *Series of an African Penguin taken at Boulders Colony:* The pictures show a bird photographed in September 1997, August 1998, January 2000 and March 2004. The penguin carries an unusual chest spot pattern that did not change during the seven years. (photos: P J Barham)

Photographs of an African penguin taken at a particular nest site at the Boulders colony show the same (unusual) plumage in the years since 1997 (see Figure 3). The pattern of spots is identical in each photograph. Other long term observations of birds with rare chest patterns, for example Figure 4, seem to back the hypotheses that the chest spot pattern of adult African penguins remains stable for lifetime.

Figure 4. *Another Series of Photos taken over Long Term:* The pictures show a bird photographed in the years 1997, 1999 and 2004. (photos: P J Barham

This extraordinary combination of visibility, uniqueness and constancy gives scope to apply biometrical techniques to the chest spot pattern in order to identify African penguins as individuals purely visually and thus non-intrusively. The aim of our system is to automatically recognize individual African penguins that present their chests to a camera device in real-time.

The following sections give a description of processing steps applied from the camera input images up to the final comparison of an extracted chest pattern against a population data base. This includes the detection of the penguin chest, the exact outlining of the chest, the extraction of the spot pattern and the finally comparison of spot patterns ∎

2. Detection of Penguin Chests

Any penguin detection system is supposed to work with footage taken in the field. Consequently, a large variety of image volatility needs to be accepted by the system including diverse lighting conditions, slight posture differences, numerous individuals, of course, and possibly changing background scenarios. The complex undertaking of finding an African penguin presenting its chest in an image of such variability made it worthy to break down this job into a sequence of subtasks following a rough-to-fine approach.

In a first instance, the original captured luminance image (see Figure 5A) is parsed for Areas of Interest (AoI's), locations that contain a penguin chest with high probability. This detection is desired to be scale invariant and robust against changes in lighting. The outcome of this phase is a set of rectangular image areas containing chest candidates (see Figure 5B).
In a second phase these AoI's are validated using several geometrical features of a penguin's chest (Figure 5C). The result of this step is a set of clearly defined chests that are delineated within the image using the upper chest outline (Figure 5D).

The next sections of this paper illustrate in detail the mechanisms that enable the system to detect and outline chests ∎
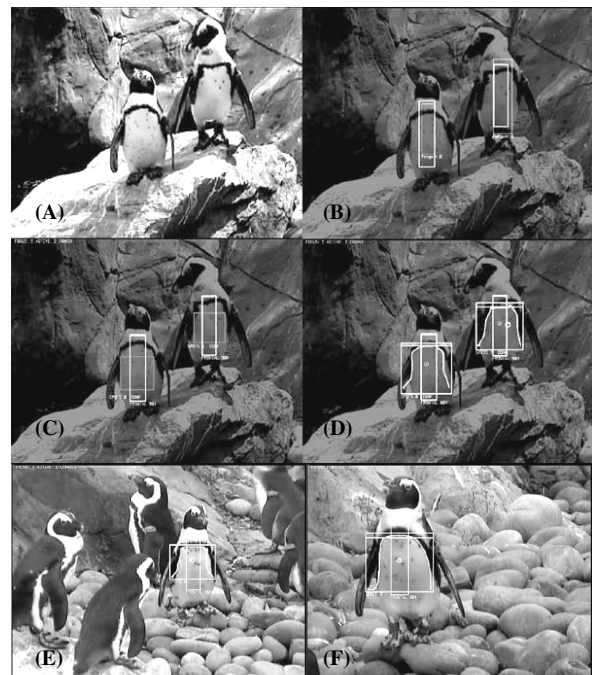

Figure 5. *Rough-to-Fine Approach to Locate a Frontal Chest:* **(A)** Original Image; **(B)** The detection of Areas of Interest clearly highlights the two penguins in the image; **(C)** Measurements for chest width and shape validate the chest candidates as suitable for further investigation. In case of video material temporal integration and tracking of the areas of interest is used to make this decision even more robust; **(D)** Detailed outlines of the chests mark the area for spot extraction clearly; **(E)(F)** Other images of automatically detected penguins in video material, the position of the birds are discovered, the chest outline is marked. (figure source [18], [19])

3. Rapid Detection of Areas of Interest

For young African penguins the black colouring of feathers including the presence of black chest spots still changes over time. Only adult members of the species carry a *stable* black and white feather pattern. For this reason, the system is supposed to identify only adult penguins to guarantee a consistent dataset.

Hence, a very distinctive characteristic that delineates only adult African penguins needed to be chosen. The black and more or less horizontal stripe in between the white neck and the chest (see Figure 6A) is a very distinctive trait that is idiosyncratic for only grown-up African penguins.

This stripe area was chosen to serve as a first discriminating area of interest (AoI) to indicate the likely presence of an adult penguin's chest. The archetypal stripe pattern stays visible to the observer for all interesting frontal positions of the bird that still fully reveal the spot configuration of the chest.

Unfortunately, the appearance of the stripe and chest area varies strongly from image to image. Different birds show different peculiarities, even when extremely rare chest configurations like the ones in Figure 3 are discounted. Together with various lighting and shadow conditions the AoI appears in all its diversity that can be viewed in Figure 6B. One can observe a variety of shapes and shadings of the stripe as well as numerous shades of the chest area.

Thus, a robust detection of the chest area requires a closer analysis of common visual features within this diversity as well as a dynamic system capability to adapt and to train the detector for different scenarios.
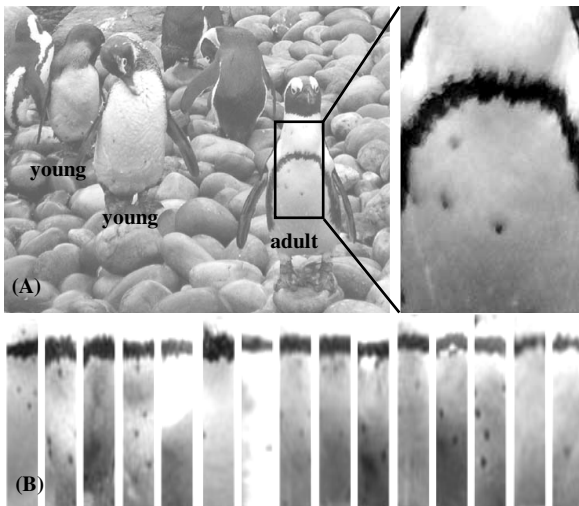

Figure 6. *Distinctive Chest Stripe of Adult African Penguins:* **(A)** Adult African penguins carry a distinctive and stable black stripe on their chest whilst young members of the species still change the colour of their chest feathers. **(B)** Various chests of adult African penguins under different lighting conditions. (figure source [19])

Definition of Fundamental Features

Our system is based on a fast up-to-date vision specific approach that performs with a high level of robustness and supports real-time processing. Its earliest version was first published by Viola and Jones for facial detection in 2001 [1]. The technique focuses on the learning of simple local luminance features like edges, lines and points (see Figure 7).

The methodology reverts to classical convolution techniques, to Heckbert's Integration-Filters [12], to Simgard's 'boxlets' [11] and to several other earlier advances. It takes the existing hardware for image processing into account and therefore purely relies on the processing of strictly rectangular image areas.

Initially, the technique was designed and successfully tested on the detection of upright human faces within greyscale images [1]. Since then, the method has been investigated and vitally improved by groups around Lienhart [2][6] and found attention by various researchers around the globe recently – mainly applying the concept to tasks of classical human recognition like facial recognition [3][4][5][8] or predestrian detection [7] for public places.

The core idea of the method is to analyse image patches $\underline{x}$ for descriptive luminance properties by finding and extracting common stable relations between the average brightness of adjacent rectangular areas r_i within the patch. These relations can be learned from a set of example patches, they can be stored and finally used to find patches with a similar 2D luminance appearance in new images.

A rectangular area r within an image patch $\underline{x}$ might be trivially defined by its top left corner combined with width and height in a quadruple *(x,y,w,h)*. A very helpful and exploitable representation (see later eq. 8) is given with a box car image r_{box} that contains value 1 in the rectangle of interest and 0 elsewhere in the patch (see Figure 13B for visual sketch).

Box Car Image

eq. 1
$$r_{box}(m,n) = \begin{cases} 1 & \begin{aligned}(m \geq x) \wedge (m < x+w) \wedge \\ (n \geq y) \wedge (n < y+h)\end{aligned} \\ 0 & otherwise \end{cases}$$
$$where \quad r = (x,y,w,h)$$

Let *S(r)* describe the average pixel value of such an area *r* within an image patch *x*. We apply fast contrast stretching to gain some invariance from changes in lighting (for parameter explanation see [2]).

Average Pixel Value ; Fast Lighting Correction

eq. 2
$$S(r) = \frac{\sum_{m \geq x}^{m < x+w} \sum_{n \geq y}^{n < y+h} \underline{x}(m,n)}{w \cdot h} \quad ; \quad \underline{\underline{x}}(m,n) = \frac{\underline{x}(m,n) - \mu}{c \cdot \sigma}$$

Several adjacent rectangular areas r_i can then be combined to form a single feature f by measuring differences of all $S(r_i)$, where the weights w_i represent the positive or negative contribution of each area.

eq. 3
Single Haar - like Feature
$$f(\underline{x}) = \sum_{i \in I} w_i \cdot S(r_i)$$

Such an image measure f is called a Haar-like feature; the naming is based on the similarity to Alfred Haar's functional decompositions using step functions [9]. Haar-like features give a quantity for the presence or absence of contrast characteristics at a specific image location. Most simple Haar-like features can be described as edge-, line- or point features as illustrated in Figure 7.

For each feature f a weak classifier k_f can be trained on a set of positive and negative samples. Any straightforward training process then outputs an optimal threshold t that separates the positives (marked as class 1) best from the negatives (class 0) where $p \in [1, -1]$ triggers the unequal sign.

eq. 4
Weak Classifier
$$k_f(\underline{x}) = \begin{cases} 1 & p \cdot f(\underline{x}) < p \cdot t \\ 0 & otherwise \end{cases}$$
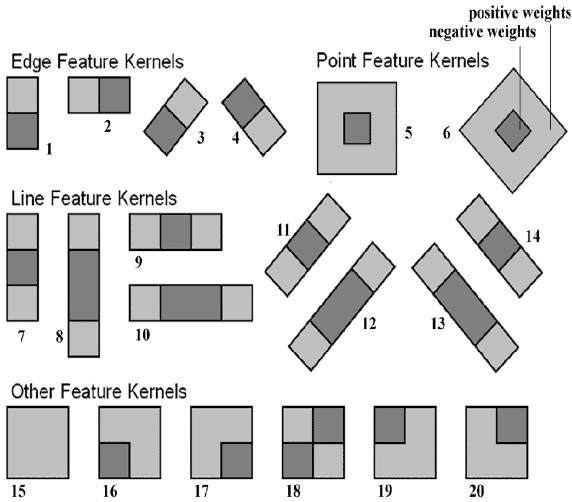

Figure 7. *Pool of Haar-Like Feature Kernels:* Brightness-relations between rectangular areas can be used to describe more complex characteristics of an image-patch. In order to reduce this feature space down to practically computable cardinalities one can focus on local interdependencies and incorporate only adjacent rectangles. The simplest features that can be constructed in this way are edge-, point- and line-features that can be found amongst the shown (incomplete) selection of Haar-like feature kernels. Whilst Viola and Jones in [1] used the feature set {1,2,7,9,18}, Lienhart in [2] changes that basic set to {1,2,3,4,5,7,8,9,10,11,12,13,14} and achieves better results. We extended this set again by adding kernel 15 in order to allow the learning of features that are not based on contrast but pure luminance appearance. (figure source[17])

Learning Essential Chest Features

Some of these classifiers k_f perform poorly but a combination of the ones working best leads to a stronger, so called 'boosted' classifier h. In this work the AdaBoost algorithm [10] is chosen to handle that task following the strategy of Lienhart [6]. It is a supervised learning approach that requires the pre-selection of several hundred positive sample patches like those in Figure 6B and another set of negative patches.

As an initial step all N image patches $\underline{x}_i$ that serve as samples get marked with a parameter y_i that is set to 1 for positive samples showing a chest and 0 for all others. In addition, a weight v_i gets assigned to each patch $\underline{x}_i$. It counts how well the so far computed classifier performs for the specific sample. The following scheme illustrates the central Discrete AdaBoost functionality:
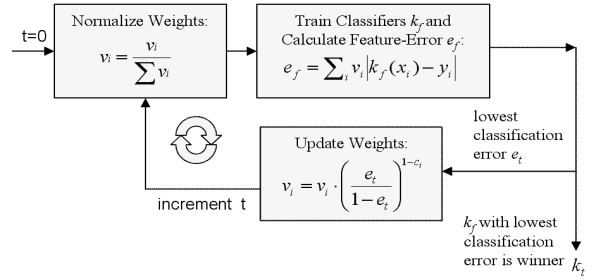

Figure 8. *Central Loop of the AdaBoost Feature Selection:* After an example preparation the evenly initialized weights get normalized in order to represent a probability distribution. In a following step, the weighted classification error e_f is calculated for **all** available unused fundamental features k_f. Based on that result the feature performing best is chosen to be the winner k_t of the loop number t with classification error e_t. Before the next loop can be performed weights for each sample are modified in order to decrease the influence and herby the importance of samples that are classified well by k_t. The supporting parameter c_i is set to the value 0 in case $\underline{x}_i$ was classified correctly by k_t and it is set to 1 otherwise. (figure source[17])

The algorithm outputs the next best weak classifier k_t together with its classification error e_t for each loop t. After T loops, once there are enough weak classifiers selected for a certain level of description detail, the learning cycle is interrupted.

A sorted sequence of weak classifiers is now available which serves to construct the final boosted classifier $h(\underline{x})$. The discriminating classifier function $h(\underline{x})$ categorizes any image patch $\underline{x}$ either as positive 1 (containing a chest) or negative 0 (no chest).

eq. 5
Strong Boosted Classifier
$$h(\underline{x}) = \begin{cases} 1 & \sum_{t=0}^{t \leq T} \alpha_t k_t(\underline{x}) \geq \frac{1}{2} \sum_t \alpha_t \\ 0 & otherwise \end{cases} ; \quad \alpha_t = \log \frac{1-e_t}{e_t}$$
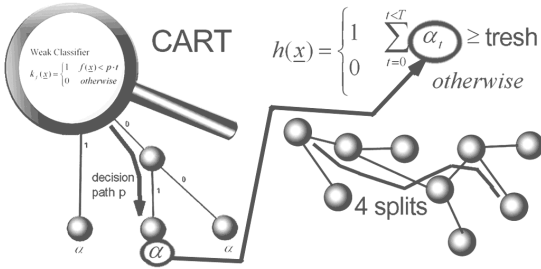
Figure 9. *CART Structures to Represent Feature Interrelations:* **(A)** As visualised above, a CART structure is a binary tree that holds already introduced weak classifiers k_f as nodes. During detection a best fitting path p within the CART is chosen for each input image sample according to the weak classifier's response to this sample. Each vertical tree path p finally terminates in a leaf. This leaf contains a weight α that characterises the positive or negative contribution of the feature combination (covering all Haar-like features that are member nodes of the path p) to the strong boosted classifier $h(\underline{x})$. As the equation in **(B)** shows, in case the sum of contributions is positive and larger than a trained threshold *tresh* the input sample is classified as positive (1) and otherwise as negative (0). **(C)** The maximal supported edge length of a path p (also called 'no. of splits') within a tree determines the capacity of the CART to represent complex interconnections between the feature nodes. As shown in [6], good results can be achieved using a maximal length parameter scaled between two and four. (figure source[17])

The technique so far uses a stump learning method that classifies on the basis of linear combinations of the fundamental Haar-like features k_f. Our system follows Lienhart's suggestion to introduce Classification and Regression Trees (CART) to prevail over this shortcoming [6].

Each input classifier for AdaBoost is remodelled as a CART structure of weak classifiers k_t instead of using plain Haar-like features. The weak classifiers are placed into an organized tree structure rather than into a sorted sequence. This ordering strategy allows the representation of non-linear interdependencies between basic classifiers using vertical tree paths (see Figure 9) ∎

Figure 10. *AoI Detector Spotting Frontal Penguin Chests:* The detector was tested on a series of black and white still images and footage. Some result images are shown above. The detector might fire several times on one and the same chest instance. (figure source [18], [19])

4. Speeding up the System

In order to apply the detection method to video streams (life camera output etc.) the extraction of the areas of interest is desired to meet real-time constraints.

Viola and Jones [1] propose the concept of attentional cascades to rapidly speed-up the detection system. The technique allows refocussing computational resources on promising image patches and discards other image regions early from any further investigation.

Therefore, the assembled CART structures are clustered into m small classifier groups, so called 'stages'. The tree classifiers with the lowest classification error are put into the first stage, respectively.

For each input image patch $\underline{x}$ a boosted classifier constructed out of the stage member's contributions α is to decide whether to go on to the next stage or to reject the patch immediately (see Figure 11).
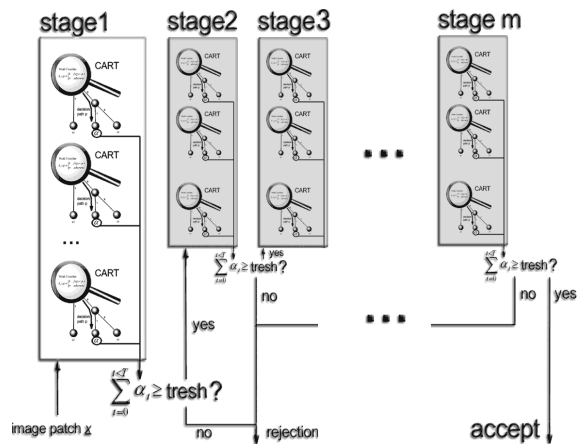

Figure 11. *Attentional Cascades for Real-Time Processing:* A collection of CART structures forms a stage. Given an input image patch $\underline{x}$ the CART structures produce their α-responses. These are summed up over the entire stage and compared to a stage threshold. This comparison decides whether the stage rejects the sample $\underline{x}$ or passes it on to the next stage. The patch is classified as positive only in case the last stage m accepts $\underline{x}$. (figure source[17])

A very early rejection of areas that do not contain a certain small number of the most essential features dramatically reduces the amount of further computation for this particular region. Only the 'more interesting' image patches are passed though for higher stage analysis (see Figure 12).

On the other hand this cascading strategy allows the removal of regions without having had a 'detailed check' combining all learned features for detection. Hence, a small increase of false negatives has to be accepted as trade-off for the vast speed advantage.
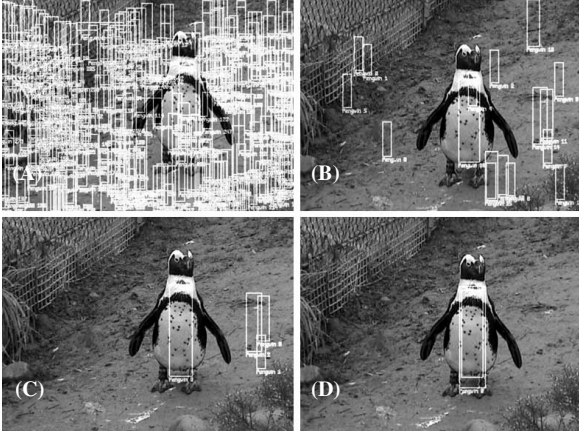
Figure 12. *Application of Attentional Cascades on Chests:* **(A)** Image areas that are accepted as likely to represent a chest after one stage are marked as white rectangles. **(B)** After three stages… **(C)** After five stages… **(D)** …and after seven stages with final result. (figure source [18], [19])

The evaluation of the rectangular sum *S(r)* used by all Haar-like features *f* is the most crucial low level computation task that is carried out thousands of times per image. Consequently, any performance optimisation of this errand has an essential effect on the overall system performance.

The computation of *S(r)* can be understood as a convolution of the image *I* with the box car image r_{box} (remember eq. 1) that defines the rectangular area.

eq. 6   Rectangular Sum as Convolution

$$S(r) = I * r_{box}$$

A fundamental integration rule for simple polynomial convolutions in case *I* and r_{box} have finite support can be used to optimize the convolution process [11][12].

     Linear Convolution

eq. 7 $(I * r_{box})^{(n)} = I^{(n)} * r_{box} = I * r_{box}^{(n)} = I^{(p)} * r_{box}^{(q)}$

     ...where $p + q = n$

This extraordinary property enables to substitute the expensive convolution of eq. 6 with an expression that needs no more than four simple additive pixel operations for evaluation (see Figure 13).

     Quick Rectangular Sum

eq. 8

$$S(r) = I * r_{box} = I^{(2)} * r_{box}^{(-2)}$$

$$S(r) = \left(\iint I \right) * \left(r_{box}'' \right) = II * \left(r_{box}'' \right)$$

$$S(r) = II(x-1, y-1) + II(x+w-1, y+h-1)$$
$$- II(x+w-1, y-1) - II(x-1, y+h-1)$$

Only the four double integrated corner pixels of the original rectangular area are enough to enable the computation of *S(r)*. This is a giant speed-up compared to *w×h* pixel accesses as given by the brute force style eq. 2.
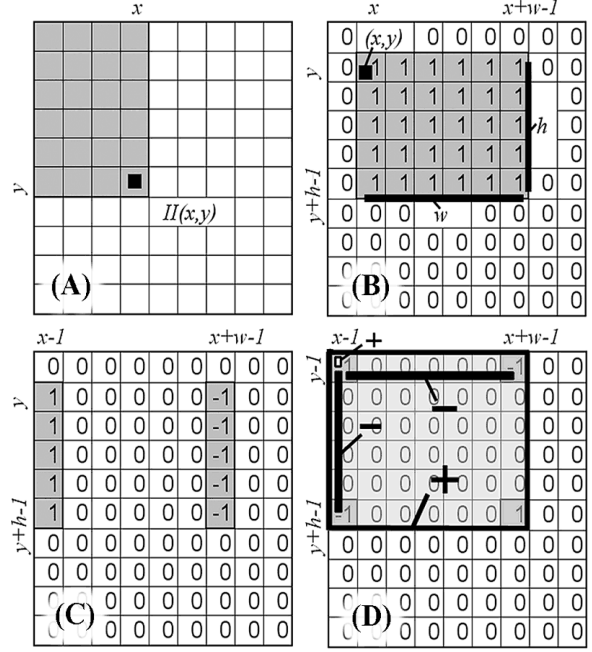

Figure 13. *Fast Rectangular Pixel Sum using the Integral Image:* **(A)** The value of the integral image *II* at a specific position *x,y* (marked in black) within an image patch <u>x</u> (shown as grid) is defined as the sum of all pixels left of *x* and above *y* (grey) in the original image I (see also eq. 9). **(B)** The box car image r_{box} is defined as 1 within the rectangular area of interest (grey) specified by *r=(x,y,w,h)* and it is equal to 0 elsewhere. **(C)** The first derivative r_{box}' is achieved by row-wise differentiation of r_{box}. **(D)** Column-wise differentiation of r_{box}' leads to r_{box}'' that contains only four corner values, 1 or –1, different from 0. This fact allows a fast convolution of *r* and *I* using *II*: The sum of pixels *S(r)* within the area of interest in the original image *I* can be computed as difference and sum of only four pixel values in the integral image *II* (see also eq. 8). These four corner values represent the sums of the marked rectangular areas in *I*. Their positive or negative contribution to *S(r)* is shown. (figure source [17])

This quality enables to rapidly evaluate rectangular features. But still, the method relies on a quickly generated discrete integral image *II*.

     Integral Image Defintion

eq. 9

$$II(x, y) = \sum_{j=0}^{j=y} \sum_{i=0}^{i=x} I(i, j)$$

Auspiciously, before the detection step is applied the calculation of the integral image needs to be done only once for the entire image.

     Rapid Integral Image Computation

eq. 10

$$II(-1, y) = 0 ;$$
$$II(x, y) = II(x-1, y) + H(x, y)$$
$$H(x, -1) = 0 ;$$
$$H(x, y) = H(x, y-1) + I(x, y)$$

It can be calculated as depicted above within linear computation complexity *O(n)* using a recursive line by line approach [1] ∎

5. Finding the Detailed Chest Outline

Each rectangular area of interest r_{AoI} needs to be examined whether it convincingly contains a chest. Therefore, a series of properties is validated around the AoI.

The measurement of the chest width w_{chest} is derived using edge detectors x_{left} and x_{right} that probe the image starting from the assumed upper chest centre point (c_x, c_y) in both the left and right horizontal direction.

Chest Width Detector

eq. 11
$$w_{chest} = x_{right} - x_{left}$$
$$x_{right} = \min(x \in N \mid 0 < x < c_x \wedge S_{edge}(x) < -\beta)$$
$$x_{left} = \max(x \in N \mid c_x < x < I_{width} \wedge S_{edge}(x) > \beta)$$
$$S_{edge}(x) = S((x, c_y, \varepsilon, \frac{h}{2})) - S((x - \varepsilon, c_y, \varepsilon, \frac{h}{2}))$$
$$c_x = x + \frac{w}{2}; \quad c_y = \frac{y + c_{stripe}}{2} + \frac{h}{4};$$
$$c_{stripe} = y + \frac{h}{\delta}; \quad r_{AoI} = (x, y, w, h)$$

where $S(r)$ is defined in eq.8 and $\varepsilon = \left\lfloor \frac{32 + w}{16} \right\rfloor$

The detectors using a Sobel-like kernel (sized $2\varepsilon \times h/2$) are introduced to find the spatially closest white-to-black change that is stronger than a dynamically computed threshold β. The AoI parameter δ depends on the average position of the chest stripe within the AoI image patch. The parameter ε was experimentally set and it is of course linearly dependent on the scaling of the chest represented by w. The detected landmarks x_{left} and x_{right} are supposed to denote the left and right boundary of the chest.
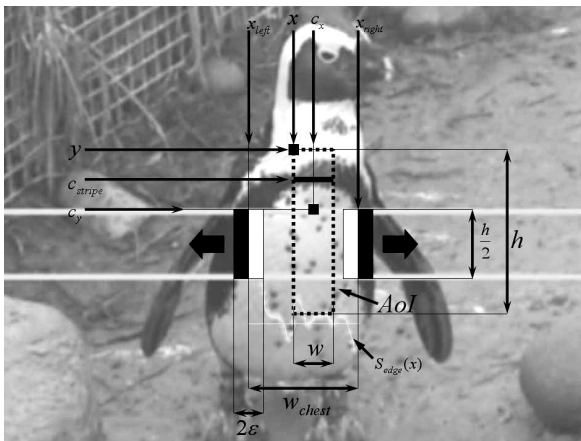

Figure 14. *Visual Description of the Chest Width Measurement:* Starting from an upper central point of the chest AoI two locally operating edge detectors moving apart search for the left and right boundary of the assumed chest. (figure source [17])

Once the chest width is derived this data can be used to verify again the correctness of the assumption that the investigated image patch really contains a chest. For this reason, the ratio of measured chest width and height of the area of interest gets compared to some proportional boundaries to guarantee an upright rectangular chest form.

Chest Width Validation

eq. 12
$$\gamma_{low} < \frac{w_{chest}}{h} < \gamma_{high}$$

The next computational phase generates the detailed chest delineation. The outline is modelled as a polygonal line P that consists of an ordered set of vertices p_i.

eq. 13 Polygonal Line
$$P = (p_1, p_2, ..., p_n); \quad p_i = (p_{i,x}, p_{i,y})$$

P is desired to stipulate the upper part of the penguin's chest boundary. Therefore, an initial approximation of the chest outline P is placed on the image using the gained information about the rough chest position.
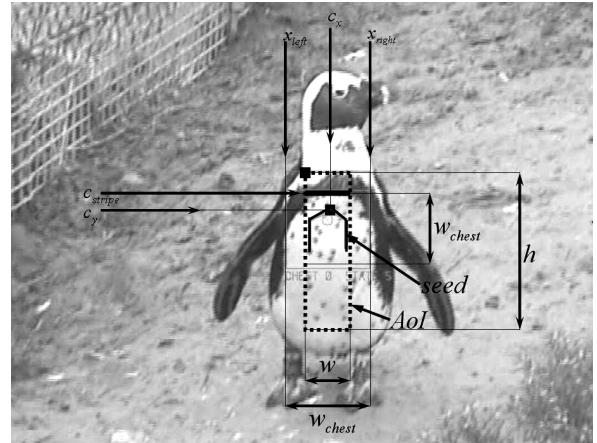

Figure 15. *Initial Outline Seed Positioning on a Penguin's Chest:* The initial polygonal seed line is positioned in the centre of the chest area as shown above where all vertices of the polygonal line are equidistant from their neighbour points. (figure source [17])

This 'seed line' gradually grows on the chest area to the chest boundary minimizing a simple energy term E based on the Euclidean distance to the chest centre C. (see Figure 16)

Distance Energy

eq. 14
$$E(p) = \frac{1}{\sqrt{(C_x - p_x)^2 + (C_y - p_y)^2}}$$
$$C_x = x_{left} + \frac{w_{chest}}{2}; \quad C_y = c_{stripe} + \frac{w_{chest}}{2}$$

Each vertex p_i of P is iteratively replaced away from the chest centre C to any available neighbourhood position that still lies on a bright chest pixel with a luminance larger than parameter τ after local lighting correction (see eq. 2).

Figure 16. *Seed Line Expansion for Stipulation of the Chest Outline:* The visualisation shows several stages of the expansion process. The polygonal line points move starting from the initial 'seed line' to the outer regions of the chest. Points cannot move to black areas as defined by the parameter τ. Hence, points move around black spots and finally terminate at the black outer chest barrier. (figure source [18], [19])

In case of very poor quality images with minimal contrast between chest area and black stripe area the polygonal line P can bleed out of the chest area.

To limit this effect P is forced to stay within a circumscribed bounding box generated with the knowledge about the chest width (see Figure 17) ∎
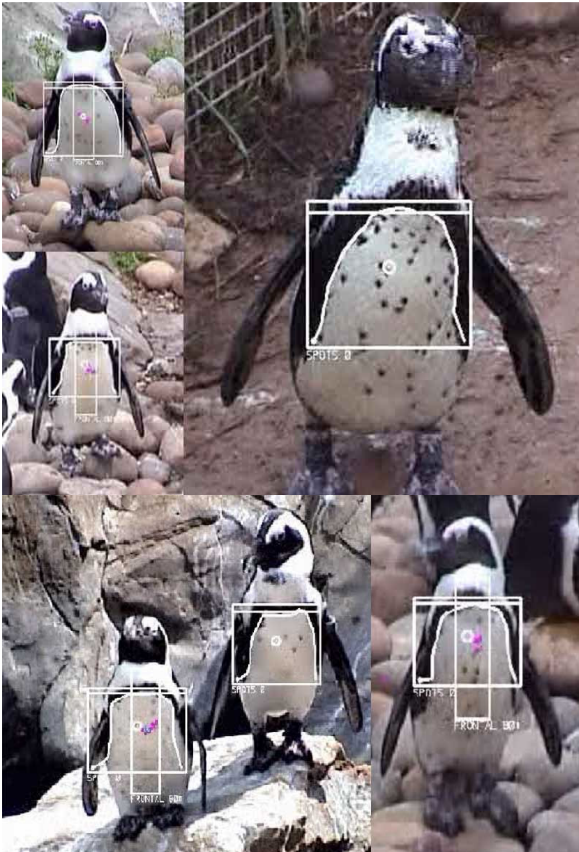

Figure 17. *Result Images with Outlined Chests of Penguins:* Screenshots of outlined penguin chests in video clips. (figure source [18], [19])

6. Extracting the Spot Pattern

The information about the exact outline of the chest enables the system to exclusively use the clearly defined upper chest area for the extraction of spots.

A direction invariant morphological gradient detector is applied to the scale normalized luminance image of the chest. The gradient image I_{grad} is obtained as the pixel-wise difference between the eroded and dilated luminance image (see Figure 18).
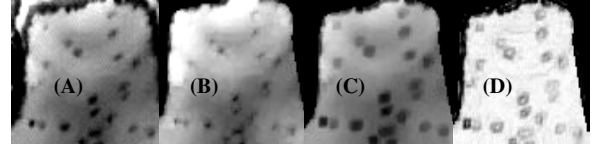

Figure 18. *Computation of the Morphological Gradient Image:* **(A)** original luminance image, scale normalized; **(B)** eroded luminance image; **(C)** dilated luminance image; **(D)** morphological gradient I_{grad} computed as difference between eroded and dilated image; (figure source [18], [19])

I_{grad} purely represents edges of the luminance image and hence, it is robust against lighting changes in the original image.

In a next step, the gradient image is convolved with a set of prototype spot kernels. The pixel values of the resulting image carry a likelihood measure that tells how an image area resembles the testing kernel. An application of a threshold to this image results in an image that contains a number of clusters of high probability for the presence of a spot.

The cluster centres are finally extracted as locations of chest spots (see Figure 19). All spot locations are gathered in a vector $\underline{s}$ containing the x-y-coordinates $s_i=(s_{i,x},s_{i,y})$ of the extracted spots ∎
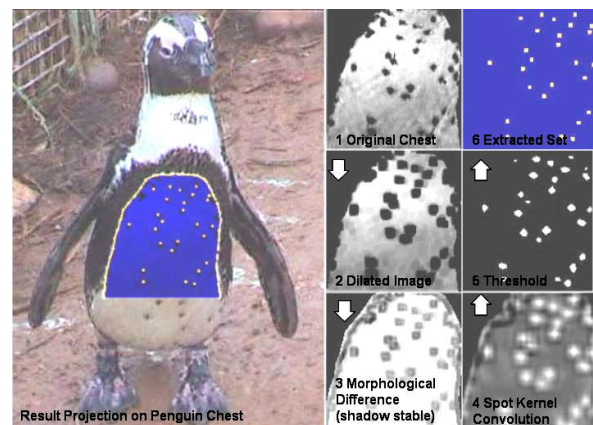

Figure 19. *Short Summary of the Spot Extraction Technique:* The visualisation shows the main phases of the extraction process. Based on the original luminance image 1 the morphological difference image 3 is computed. This image is convoluted with prototype spots and results in the likelihood map 4 for spot appearance. The cluster centres of the thresholded image 5 finally stipulate the assumed positions of the spots shown in image 6. (figure source [18], [19])

7. Comparison of the Spot Pattern

The vector $\underline{s}$ holds the coordinates of the spots in form of x-y-positions of the scale normalized image. A comparison at least requires independence in terms of translation and rotation.

A form of the Procrustes algorithm is applied to generate comparable patterns.

In a first instance, the outline centre $c_{outline}$ is computed as the average of all outline points.

eq. 15 Outline Centre

$$c_{outline} = (x_{outline}, y_{outline})$$

$$x_{outline} = \frac{\sum_{p_i \in P} p_{i,x}}{|P|}; \quad y_{outline} = \frac{\sum_{p_i \in P} p_{i,y}}{|P|}$$

All entries s_i of vector $\underline{s}$ are sorted into a new vector $\underline{u}$ by the Euclidean distance d_i to the outline centre $c_{outline}$.

eq. 16 Distance to Outline Centre

$$d_i = \sqrt{(s_{i,x} - x_{outline})^2 + (s_{i,y} - y_{outline})^2}$$

Entries $u_i = (u_{i,x}, u_{i,y})$ of vector $\underline{u}$ can serve as reference points $p_{ref} = (x_{ref}, y_{ref})$ for comparison. The reference point stipulates the origin of the comparison. It offers more stability than any centre point because it stipulates an actually measured spot position.

The first entries of $\underline{u}$ being closest to $c_{outline}$ are used first as reference points. This offers a high probability to choose the same reference spot *early* for two measurements of one and the same penguin.

In a next phase, vector $\underline{s}$ is transformed into a polar system starting with the first reference point and going on to others later if no match is found.

Polar Transform of Chest Pattern

eq. 17 $s(x, y) \xrightarrow{\text{Polar Transform}} s(\varphi, r)$

$$s(x, y) = r(\cos\varphi + i\sin\varphi)$$

$$\varphi = \arctan\left(\frac{(y - y_{ref})}{(x - x_{ref})}\right)$$

$$r = \sqrt{(x - x_{ref})^2 + (y - y_{ref})^2}$$

The entries s_i of vector $\underline{s}$ can now be sorted by r that carries the distance to the reference point. Quicksort can be applied and solves the problem fast in *O(nlog(n))*.
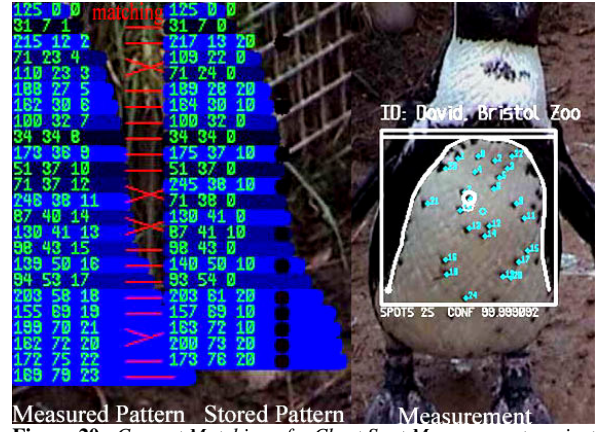

Figure 20. *Correct Matching of a Chest Spot Measurement against a Stored Pattern:* The extracted spot pattern (shown on the right, reference spot with white circle) can be used to generate a sorted identifier (left). It gets compared against a stored identifier (middle). Found matches are shown as lines between the measured and stored identifier. As visible, cross-matchings occur and even the number of extracted spots varies. (figure source [18], [19])

Once a spot pattern is transformed into this sorted vector it has the quality of a unique identifier. It can be stored as $\underline{s}_{stored}$ in the database or it can be compared as $\underline{s}_{measured}$ to any database entry.

Skin distortions and misdetections of faded spots or spots in border areas cause the extracted pattern to vary. Any exact matching technique cannot be applied.

Using the fact that spots around the chest centre are most stable against distortions and misdetections spots are linearly weighted by their vector position. Spots nearer the centre are granted higher weights. This produces an advantage for the applied method compared to other matching strategies like Hausdorff Distances.

For each member of $\underline{s}_{measured}$ the system tries to find an entry with similar angle φ at a position in $\underline{s}_{stored}$ close to the previous matching. Cross-matchings are allowed (see Figure 20), multiple matchings are tried to be resolved in the close neighbourhood.

Each entry in $\underline{s}_{measured}$ with an assigned matching in $\underline{s}_{stored}$ gets rewarded its weight. The sum of all weights is compared to an experimentally set threshold to determine a match or mismatch. In case of a mismatch the next reference point is applied. In case all reference spots are used $\underline{s}_{measured}$ and $\underline{s}_{stored}$ do not match.

The prototype detection system has been successfully applied to a small number of African penguins situated at Bristol Zoo, United Kingdom, using hand cameras for footage generation. Further experiments including automatic cameras and larger numbers of individuals are necessary to be carried out in a next project stage ∎

---

8. Conclusions and Future Work

So far, the introduced system is a prototype version that needs further testing to be applied to larger populations of African penguins. Tests within a small Zoo population with hand cameras are not satisfactory to back a large scale application from scratch. Nevertheless, we have shown, practically and technically, that there is now a working approach to identify African penguins by their chest pattern. Further experiments and improvements of the system for partial pattern detection and non-frontal images are intended to lead to long term and large scale applications of the method in the wilderness using a central pattern database server for international synchronisation of pattern data. As shown, the system does not work for young African penguins that change their feather pattern and it does either not work for penguins with extraordinary patterns like the one in Figure 3.

Figure 21. *Hypothetical System Design for a Central ID System*

A test scenario using automatic cameras will be installed at Bristol Zoo soon to get exact performance data of the system in a field experiment.

Furthermore, the technique might be applied to other penguin species, like Magellanic Penguins, Humboldt Penguins or Galapagos Penguins, that also carry spot patterns on their chest. Also the outline of the chest seems to be a unique body pattern as well that needs further investigation to serve as identifying pattern. Additionally, a system extension for tracking of individuals in groups might lead to data for behavioural analysis. There is large potential for further system development ∎
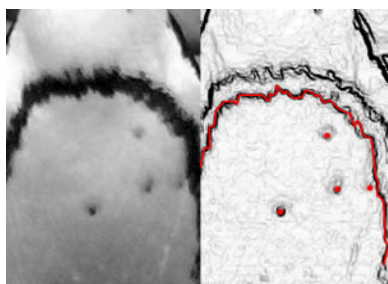

Figure 22. *Some possible Extensions of the Identification Method:* Chest and gradient image of the chest reveal the uniqueness of the chest outline. (penguin photos by Brian Lockett, Mike Bingham, Blossom Gervacio, Tilo Burghardt; figure source right [18], [19])

References

[1] *P. Viola, M. Jones. "Robust Real-time Object Detection."* Second International Workshop on Statistical and Computational Theories of Vision, Vancouver/USA, July 2001.

[2] *R. Lienhart, J. Maydt.* "An extended set of Haar-like Features for Rapid Object Detection." In Proc. of the IEEE Conference on Image Processing (ICIP'02), New York, September 2002.

[3] *P. S. Carbonetto.* "Robust Object Detection Using Boosted Learning." Department of Computer Science, University of British Columbia, Vancouver, April 2002.

[4] *Z. Zhang, L. Zhu, S.Z. Li, H.J. Zhang.* "Real-Time Multi-View Face Detection." Chinese Academy of Science / Microsoft Research Asia, Beijing, February 2002.

[5] *P. Viola, M.J. Jones. "Fast Multi-View Face Detection."* Mitsubishi Electric Research Labs, demonstration at the IEEE Conference on Computer Vision and Pattern Recognition (CVPR'03), June 2003

[6] *R. Lienhart, A. Kuranov, V. Pisarevsky.* "Empirical Analysis of Detection Cascades of Boosted Classifiers for Rapid Object Detection." In Proc. of the German 25th Pattern Recognition Symposium (DAGM´03), Magdeburg/Germany, September 2003.

[7] *P. Viola, M.J. Jones, D. Snow.* "Detecting Pedestrians Using Patterns of Motion and Appearance." In Proc. of the 9th IEEE International Conference on Computer Vision (ICCV'03), Nice/France, October 2003.

[8] *J. Barreto, P. Menezes, J. Dias.* "Human-Robot Interaction based on Haar-like Features and Eigenfaces." Institute of Systems and Robotics, University of Coimbra, Portugal, In Proc. ICRA '04, April 2004.

[9] *A. Haar.* "Zur Theorie der orthogonalen Funktionssyteme. / On the Theory of Orthogonal Functional Systems." PhD Dissertation, University of Göttingen/Germany, August 1909.

[10] *Y. Freund, R. E. Schapire.* "A Decision-theoretic Generalization of Online Learning and an Application to Boosting." In Computational Learning Theory, Eurocolt 1995, pp. 23–37. Springer-Verlag, 1995.

[11] *P. Y. Simard, L. Bottou, P. Haffner, Y. L. Cun.* "Boxlets: A Fast Convolution Algorithm for Signal Processing and Neural Networks." In M. Kearns, S. Solla, and D. Cohn, editors, Advances in Neural Information, Processing Systems, volume 11, pages 571–577, 1999.

[12] *P. S. Heckbert.* "Filtering by Repeated Integration." Computer Graphics, vol. 20, no. 4, pp. 315-321, August 1986.

[13] *L. Itti, C. Koch, E. Niebur.* "A Model of Saliency-Based Visual Attention for Rapid Scene Analysis." Chinese Academy of Science / Microsoft Research Asia, Beijing, February 2002.

[14] *M. Renner.* "Survival of Little Penguin Chicks." MSc Theses, Dept. of Zoology, University of Otago, Dunedin, April 1998.

[15] *B. Stonehouse.* "Penguin Banding: Time for Reappraisal?" Scott Polar Research Institute, University of Cambridge, Lensfield Road, Cambridge CB2 1ER, United Kingdom, 1999.

[16] Software Package; Open Computer Vision Library C++. http://sourceforge.net/projects/opencvlibrary

Other Image Sources

[17] [18] [19] *T. Burghardt.* Own Figures and Images, July 2004. / Photographs of African Penguins taken at Bristol Zoo, Bristol, UK, 2004. / Screenshots of "ID-Pen", Software Prototype for Identification of African Penguins, August 2004.

[20] *P. J. Barham.* Photographs, 1997-2004.

Thanks to Bristol Zoo for their active support.